New Covalent Salts of the 4+ V Class For Li Batteries

L. Niedzicki[2], S. Grugeon[1], S. Laruelle[1], P. Judeinstein[3], M. Bukowska, J. Prejzner[2], P. Szczeciński[2], W. Wieczorek[2], M. Armand[1]

[1]*Université de Picardie Jules Verne, Laboratoire de Réactivité et de Chimie des Solides, 33 Rue Saint-Leu, F-80039 Amiens Cedex, France*

[2]*Warsaw University of Technology, Faculty of Chemistry, 00-664 Warszawa, Noakowskiego 3, Poland*

[3] *Institut de Chimie Moléculaire et des Matériaux d'Orsay (UMR 8182), Bâtiment 410 Université Paris-Sud, F-91405 Orsay Cedex, France*

Abstract:

There urgent action required for replacing $LiPF_6$ as a solute for Li-ion batteries electrolytes. This salt, prone to highly-Lewis acidic PF_5 release and hydrolysis to HF is responsible for deleterious reaction on carbonate solvents, corrosion of electrode materials leading to safety problems then release to toxic chemicals. The only advantage of this salt is its protection of aluminium positive electrode current collector. Most attempts to replace $LiPF_6$ with hydrolytically-stable salts have been unsuccessful because of Al corrosion.

We present here two "Hückel" type salt, namely lithium (2-fluoroalkyl-4,5-dicyano-imidazolate); fluoroalkyle = CF_3 (TDI), C_2F_5 (PDI) with high charge delocalization. These thermally stable salts give both appreciably conductive solutions in EC/DMC (> 6 $mS{\cdot}cm^{-1}$ at 20°C) with a lower decrease with temperature than $LiPF_6$. Non fluorinated lithium (4,5-dicyano-1,2,3-triazolate) is comparatively less than half as conductive. The Lithium transference number T_+ measured by PFG-NMR is also higher. Voltammetry scans with either platinum or aluminium electrodes show an oxidation wall at 4.6 V *vs.* Li^+:Li°. These two salts are thus the first examples of strictly covalent, non-corroding salts allowing 4^+V electrode material operation. This is demonstrated with experimental $Li/LiMn_2O_4$ cells as beyond the third cycles, the fade of the three electrolytes were quasi-identical, though LiPF6 had a sharper initial decrease.

Keywords: lithium salt, nonaqueous electrolyte, Li-ion battery, Hückel anion

Introduction:

The electrolyte is arguably the most critical component in batteries, as it should maintain its functions in contact with both the reducing negative electrode and oxidizing positive. This is especially true for lithium batteries where a 4+ V voltage span inevitably depends on the metastability of the electrolyte versus at least one electrode. Great hopes now rest on these batteries, beyond their undeniable success in nomadic electronic, with scale-up to a progressive electrification of transportation modes to EVs, HEVs and plug-in HEVs. Most of the research effort came after the first practical "Lithium-ion" (LIB) technology in 1991, where Li^+ is shuttled between two intercalation compounds, now established mainly as graphite (-) and cobalt-based layered oxides (+), manifestly the most extreme voltages that can be operated "safely", though the list of incidents due to runaway reactions becomes alarmingly longer with @ 10^9 batteries in operation. The miracle(s) taking place within batteries 10-100 g is unlikely to scale-up for the 200 Kg of an EV. Mixture of carbonates, and $LiPF_6$ as solute are used in the quasi-totality of LIBs because of their high conductivity, but the determining factor is the absence of corrosion of aluminium current collectors at high anodic voltages (> 4.5 V *vs.* Li^+:Li°), i.e. well beyond the thermodynamic potential (1.3 V), and no other metal can offer a substitute in terms of cost, weight and malleability. The drawbacks of $LiPF_6$ are severe: i) the high conductivity is relative as the transport number is low [1]; ii) the tendency to dissociate into LiF and PF_5 with the latter inducing cationic chemistry deleterious to electrolyte; iii) the facile hydrolysis to HF, inducing corrosion of the cathode materials, for instance Mn dissolution in $LiMn_2O_4$. The leached-out species after diffusing to negative electrode modify the SEI, raising its impedance, with resulting overheating and dramatic safety issues; iv) combustion releases copious amount of HF; v) less spectacular than a fire, smouldering, i.e. the reaction at high temperature with ethylene carbonate yields a derivative of fluoroethanol, a family of exceedingly toxic (LD 50 = 0.5 mg/kg in mice) chemicals [2].

Of the possible substitutes for $LiPF_6$, none of the classical $LiAsF_6$, $LiSbF_6$, $LiClO_4$ are close to meeting safety or innocuousness requirement. The "designer" anion $[(CF_3SO_2)_2N]^-$ developed for polymer electrolytes (now also successful as ionic liquid component) would be

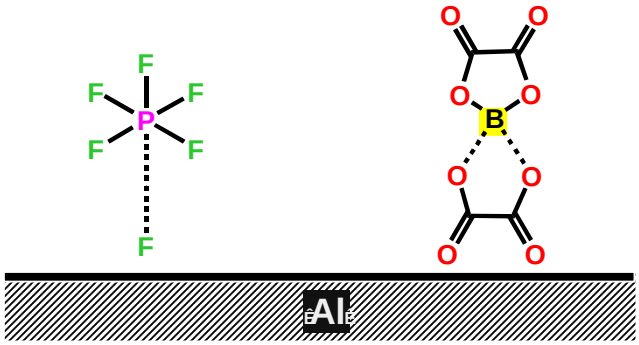

Figure 1. Scheme of Al passivation with labile coordination salts.

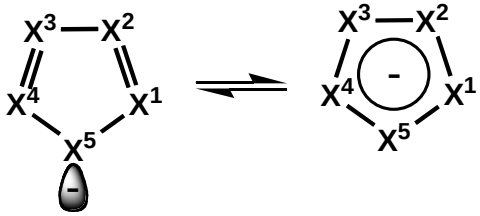

Figure 2. The structure of "Hückel" anions: X = N, CCN, CCR_F…

ideal, except its crippling lack of aluminium protection. Conversely, the coordination anion, (bisoxalato)boron (BOB) ion, does passivate aluminium, but oxidises with gas evolution (CO_2) specially above room temperature. Besides, the high rigidity/bulk of the molecule induces unfavourable phase diagrams at low temperature. Conventional wisdom suggests that the lability of F^- and $C_2O_4^{2-}$ from PF_6^- resp. BOB^- is the reason for passive film formation (Fig. 1). A promising substitute for $LiPF_6$ is $Li[FSO_2NSO_2F]$ (LiFSI) which does not corrode aluminium up to at least 4V. The cleavage of the S–F bond, (though more covalent than P–F) suggests that the passivating layer on Al is AlF_3, a compound with high lattice energy, and used in microelectronics to protect Si for F-plasma etching. In similarity, the oxalate anion whose chelate "pincer" gap is more adapted to Al than B radii, would adsorb also (Fig 1).

The question thus is the existence of a truly covalent anion, not prone to hydrolysis and irreversible HF, yet able to form a passivating layer on Al°, or at least preserve the native Al_2O_3 layer. Several years ago, we have introduced the concept of "Hückel anions" [3] (Fig 2), i.e. the delocalization of 6 "π" electrons on an aromatic 5-membered ring. A wealth of compounds with ring nitrogen a and/or CN in the periphery [4,5] have been modelled and show very weak Li^+-anion interactions, especially as the CN substitution increases. The simple representative,

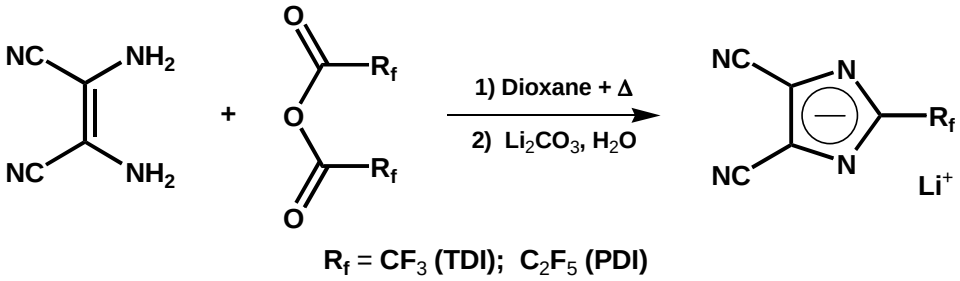

Figure 3. Synthesis scheme for LiTDI and LiPDI.

4,5-dicyano-1,2,3-triazole (DCTA) has favourable conductivities in PEO electrolytes [6]. To further increase the resistance to oxidation and lessen the ion-pair formation, replacement of central N by C–CF_3 or C_2F_5 to 4,5-dicyano-2-trifluoromethyl-imidazole and 4,5-dicyano-2-pentafuoroethyl-imidazole (TDI and PDI respectively) has, also in PEO electrolytes, showed excellent conductivities and favourable phase diagram. No oxidation was seen before the polyether own limit (4V) [6]. We inferred that these salts deserved further investigation in classical liquid electrolytes, as a covalent salt is of considerable technological advantage, without the release of a strong Lewis acid like PF_5 able to wreak chemical havoc in the solvent and avoid the formation of fluoroethanol derivatives, a threat unacceptable for general application of EVs. These salts will be compared with the non-fluorinated LiDCTA and $LiPF_6$.

Experimental:

TDI and PDI are made in a one-pot reaction from commercial chemicals (Fig. 3) [7,8]. The two white powders were dried at 150 °C for12 hours in a Büchi TO-50 oven prior to being used and kept in a dry box. LiDCTA was made from the reaction of diamino-maleonitrile with *tert*-butyl nitrite in diethyl ether at 0°C for 48 hours. The turbid yellow suspension was centrifuged and stripped from solvent. Crude 4,5 dicyano imidazole was sublimed in vacuum (80 °C) to obtain the pure acid. The Li salt was made in ethanol by reaction on 10% excess of Li_2CO_3, filtration and drying. $LiPF_6$ 1M in EC/DMC (50/50 w/w) was obtained from Merck (LP30®).

Coupled Thermogravimetric and DSC traces between RT and 300°C under a constant flow of argon (50 ml min^{-1}) were acquired with a Netzsch Jupiter STA 449C thermal analyser at a heating/cooling rate of 10 °C min^{-1}. The isothermal drift and sensitivity values are 0:6 g h^{-1} and 0:1 g, respectively. Aluminium crucibles were loaded with 25 mg of the salts and sealed in the

dry box. A small hole was punched in the lid just prior to loading in the apparatus.

Conductivity measurements were performed using a CDC749 (Radiometer Analytical) cell. All the electrochemical experiments were conducted at 20 °C using a VMP3 system (Biologic Science Instruments) with a 1 M lithium salt dissolved in EC/DMC (50/50 w/w) solvents mixture.

PFG-NMR diffusion measurements were carried out on 9.4 T Bruker Avance 400 NMR spectrometer equipped with a Bruker 5 mm broadband probe with a z-axis gradient and a temperature controller (stability and accuracy 0.2 °C). NMR resonance frequencies are 400.1 MHz, 376.50 MHz and 155.51 MHz respectively for ^{1}H, ^{19}F and ^{7}Li nuclei. The self-diffusion measurements were performed with the pulsed field gradient stimulated echo and LED sequence using 2 spoil gradients (PFG NMR) [9]. The magnitude of the pulsed field gradient was varied between 0 and 40 G·cm^{-1}, the diffusion time Δ between two pulses was fixed at 100 ms and the gradient pulse duration δ was set between 3 ms and 10 ms depending on the diffusion coefficient of mobile species. This allowed us to observe the attenuation of spin echo amplitude over a range of at least 2 decades leading to a good accuracy (<5 %) of the self-diffusion coefficient values. They were determined from the classic relationship $A/A_0 = \exp(-Dg^2\gamma^2\delta^2(\Delta - \delta/3))$ where g is the magnitude of the two gradient pulses, γ is the gyromagnetic ratio of the nucleus under study and A and A_0 are respectively the area of the signal obtained with or without gradient pulses.

Cyclic voltammetry measurements were acquired at a scan rate of 30 mV s^{-1}, in the 0.5-6 V or 0.01-6 V potential ranges (*vs.* Li^+:Li°). An Al or Pt wire was used as working electrode, a Pt wire as counter electrode and metallic Li as reference electrode.

Galvanostatic tests were performed in Swagelok® cells using a plastic positive electrode on an Al disk containing 64 wt % $LiMn_2O_4$, 8 wt % SP carbon, and 28 wt % poly(vinylidene fluoride)-co-hexafluoropropylene (PVdF-HFP) copolymer binder (the electrode films were cast and processed using a procedure previously reported) [10], a 1 cm disk of Li foil as the negative electrode, and a Whatman GF/D borosilicate glass fibre mat separator. The electrode rate capability was determined via the collection of a signature curve as the function of the salt. After a low rate charging, the cell was successively discharged at decreasing rates (5C, 2.5C, 1C, 0.5C, C/5, C/10 and C/20) with a relaxation time of 30 min between each step.

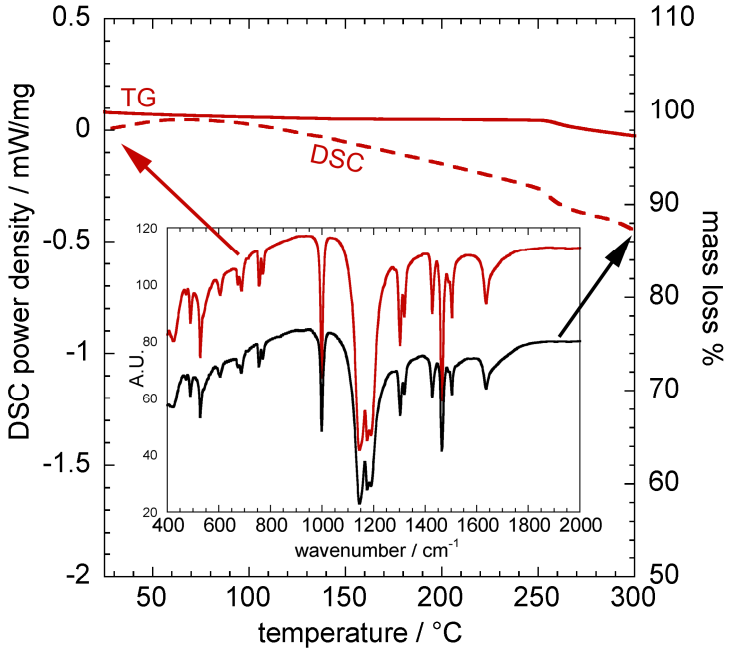

Figure 4. TGA, DSC traces of LiTDI, heating scan at 10°C mn^{-1} and IR spectra recorded before and after the scan.

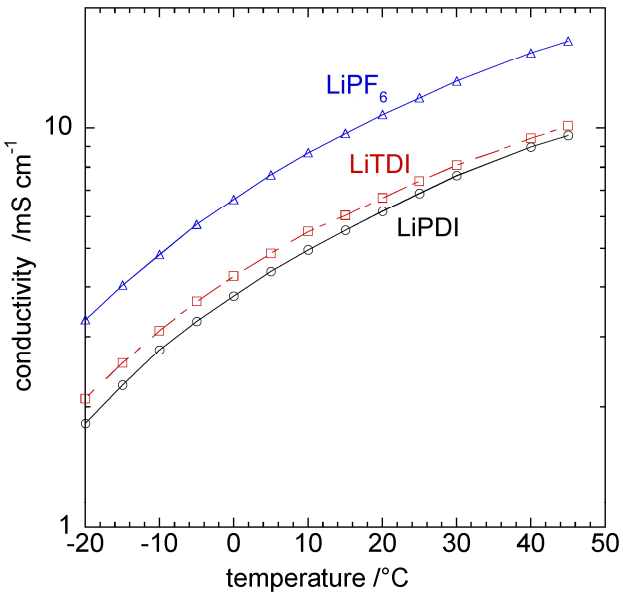

Figure 5. Conductivity of 1M $LiPF_6$, LiTDI and LiPDI salts in EC/DMC (50/50) as a function of the temperature.

Results and discussions:

The two salts TDI and PDI are stable up to 250 °C as shown by TGA-DSC. The TDI salt IR spectra recorded on the material dried at 150°C and 300°C are identical as shown in Fig. 4, showing that the material is chemically stable; PDI, (not shown) behaves similarly. 1 M solutions were prepared from EC/DMC (50/50 w/w) mixture inside the dry box. Karl-Fisher measurements performed on the solution showed a water content of 20 ppm, when the drying temperature was 150 °C and this treatment was kept for all batches used in this study except $LiPF_6$.

The conductivity of such solutions was measured at 20°C and is summarized in table 1: for comparison, LiTFSI, dicyanotriazole (DCTA) anions salts were measured. The TDI and PDI salts display quite similar conductivities in the [-20 +45 °C] temperature span (Fig 5). The lower activation energy of TDI and PDI vs. $LiPF_6$ makes them more suitable for low temperature applications. These salts are much more conductive than DCTA, with only $LiPF_6$ and LiTFSI showing higher performances, and comparable with LiBOB (@ 7.5 $mS{\cdot}cm^{-1}$ at 0.7 M).

Solute	σ ($mS.cm^{-1}$)
$LiPF_6$	10.8
LiTFSI	9.0
LiTDI	6.7
LiPDI	6.3
LiDCTA	2.7

Table 1. Conductivity of various salts 1M in EC/DMC 50/50; T = 20°C.

The Vincent & Bruce polarization for T_+ estimation [11] relies on the hypothesis that this value is independent of concentration and assimilates activities with concentrations. The NMR measurement of transport numbers is immune to such criticism, as no chemical gradient is created. The diffusion coefficients obtained by PFG-NMR for the different transport numbers are summarized in table 2 and the cationic transport numbers are calculated by definition as $T_+ = D_{cation} / (D_{cation} + D_{anion})$ assuming the validity of the Nernst-Einstein equation. Table 2 contains also the diffusion coefficients for the two components of the solvent (^{1}H NMR resonances of linear DMC and cyclic EC are respectively at 3.3 and 4.2 ppm).

	D_{cation} (cm^2s^{-1})	D_{anion} (cm^2s^{-1})	$D_{solvent}$ (cm^2s^{-1})	T_+
$LiPF_6$ (LP30®)	$2.45 \cdot 10^{-6}$	$3.50 \cdot 10^{-6}$	$4.59 \cdot 10^{-6}$ (EC) $5.97 \cdot 10^{-6}$(DMC)	0.41
LiTDI	$2.21 \cdot 10^{-6}$	$2.57 \cdot 10^{-6}$	$4.59 \cdot 10^{-6}$ (EC) $5.79 \cdot 10^{-6}$ (DMC)	0.46
LiPDI	$2.14 \cdot 10^{-6}$	$2.53 \cdot 10^{-6}$	$4.82 \cdot 10^{-6}$ (EC) $6.36 \cdot 10^{-6}$ (DMC)	0.46

Table 2. PFG-NMR diffusion coefficients for Li^+, anion, EC and DMC and transport numbers for Li^+; T = 25°C.

As can be seen from this data, the transport number of lithium cations with both TDI and PDI anions are higher than that for PF_6^-. The larger diffusion coefficient for the less polar DMC solvent is a favourable feature, this faster moving molecule leaving behind high- ε EC, a better solvent for concentrated salt solutions at the negative (on discharge) and positive (on charge). It is interesting to note that the T_+ value is the same for both TDI and PDI, despite the larger volume of the latter. This, once again, shows that the relative mobilities of anions are determined by their chemical structure and charge delocalization as was showed earlier in the $Li[R_fSO_3]$ and $Li[(R_fSO_2)_2N]$ ($R_f = C_nF_{2n+1}$, $1 \leq n \leq 4$) systems [12,13] independently on their size. The role of the anion in the close environment of the cation is also reflected by the different chemical shifts of Li^+, $\delta = -0.81, -0.46$ and -0.58 ppm for PF_6^-, TDI and PDI respectively.

The voltage stability window of the electrolyte had been tested on Pt electrode as shown in Fig. 6-a. The supporting solvents are stable or metastable to @ 6V over the short time of the cyclic voltammetry and the PDI and TDI anions show good stability until 4.80 V *vs.* Li^+:Li° followed by an oxidation wall which is similar for both anions, reflecting the similar electronic structure of the charge-bearing ring.

When Pt is replaced by an aluminium wire (Fig. 6b), TDI (and PDI not shown for clarity) oxidize at about the same potential of 4.75 V, and the current before this threshold and the return current are negligible, almost similar to that found for $LiPF_6$ in commercial LP30®. For comparison, LiTFSI undergoes a large corrosion current beyond 3.3 Volts, practically an order of

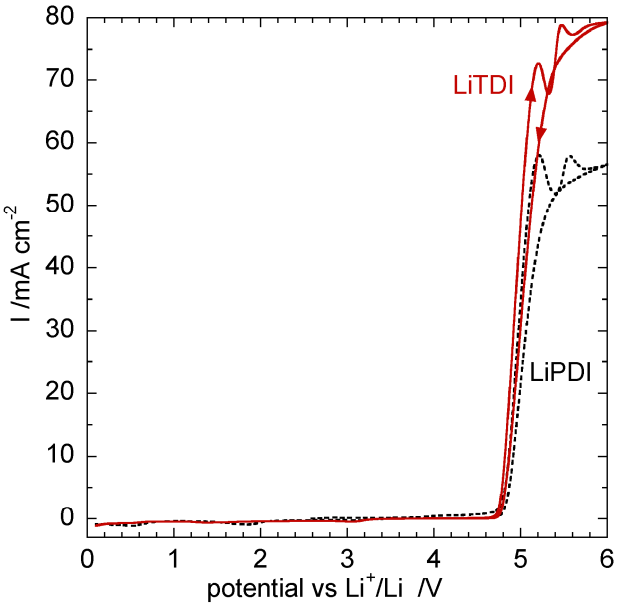

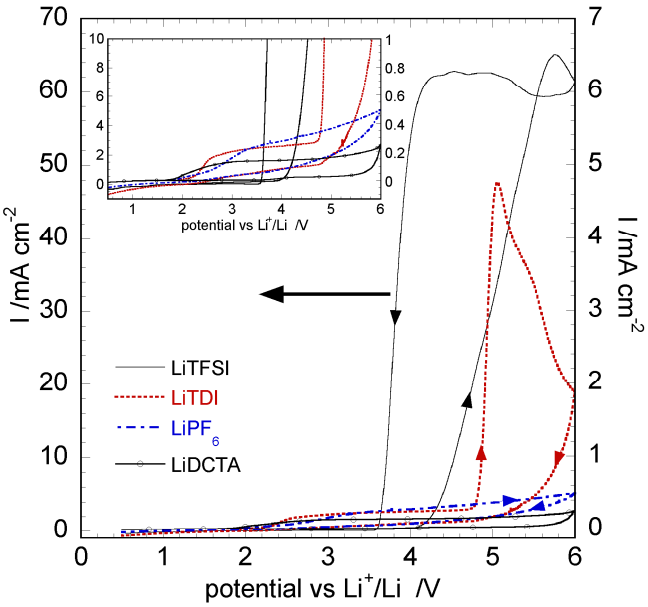

Figure 6. a) Cyclic voltammogram of 1M LiTDI and LiPDI in EC/DMC (50/50 w/w), on Pt electrode at 30 mV·s^{-1}, upper cut-off 6 V (*vs.* Li$^+$:Li°).

b) Cyclic voltammogram of LiTDI, $LiPF_6$, $Li[CF_3SO_2)_2N]$ and LiDCTA, all 1M in EC/DMC (50/50), on Al electrode. Voltage limits are 0.1-6V (*vs.* Li$^+$:Li°), scan speed 30 mV·s^{-1}.

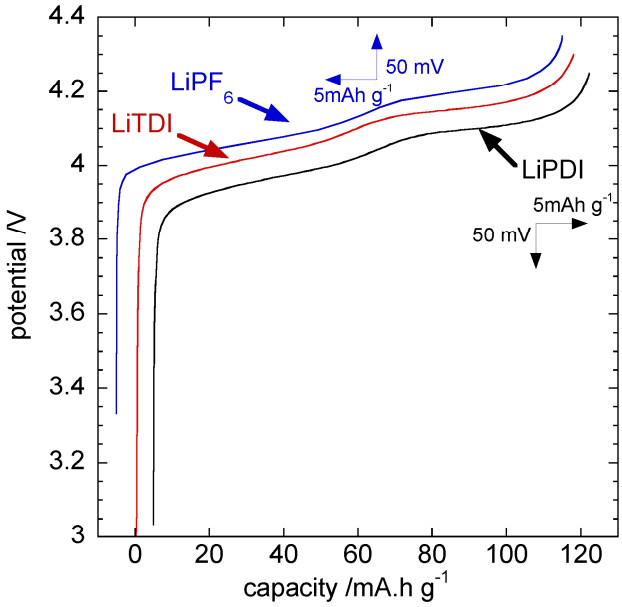

Figure 7. Charge behaviour for $LiMn_2O_4$ with LiTDI, LiPDI and $LiPF_6$, all 1M in EC/DMC (50/50); upper cut-off 4.3 V. For legibility, LiPDI and $LiPF_6$ traces are shifted by 5 mAh.g^{-1} and 50 mV.

magnitude larger than the oxidation wall of TDI. LiDCTA was also tested, and shows also very little corrosion up to 6V. Thus the three Hückel rings, (≠ $LiPF_6$), either passivate the Al surface, or keep intact the native Al_2O_3 layer on this metal and are the first totally covalent anions showing this necessary property. The absence of dissolution of native Al_2O_3 probably applies to PDI and TDI, while DCTA anion, devoid of electron-withdrawing fluorine, is calculated to oxidize ≈ 4V *vs.* Li^+: Li° and thus the low current is attributed to an insoluble protecting layer.

When a Swagelok® cell laden with 7 mg of $LiMn_2O_4$, and carbon is charged (C/20) to 4.3 V (Fig. 7) the theoretical capacity for this voltage upper limit is obtained (≈ 120 mAh·g^{-1}) with both salts, without any visible side reactions for the electrochemical delithiation. The knee at 4.1 V is typical of Li^+ ordering in the spinel structure (x ≈ 0.5 in $Li_xMn_2O_4$).

The cycling behaviour at C/10 was compared between LiTDI, LiPDI and LP30 electrolytes in the same Swagelok cells. As evident from figure 8, the cells behave quite promisingly, with a fade on the first 25 cycles at an average of 3 % per cycle, as compared with 5 % for $LiPF_6$ in the same conditions, though the initial capacity with $LiPF_6$ was slightly higher. It

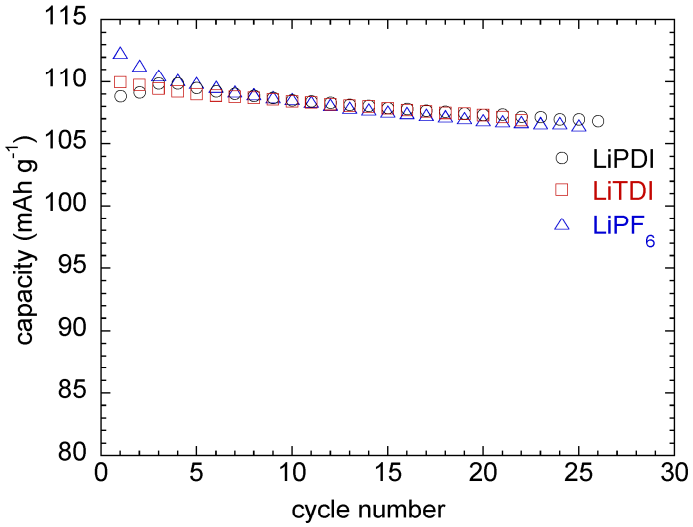

Figure 8. Discharge capacity retention of $LiMn_2O_4$ electrode with 1M LiTDI, LiPDI and $LiPF_6$ in EC/DMC (50/50); upper/lower cut-off 4.3/3.5 V (*vs.* Li^+:Li°).

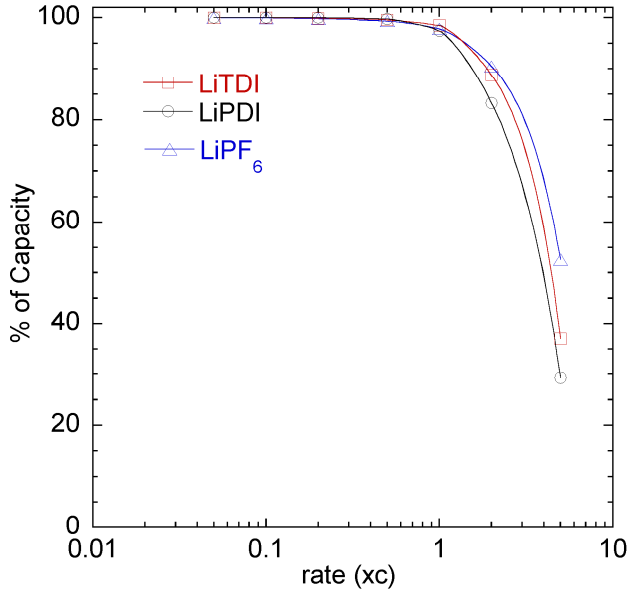

Figure 9. Signature curve of $LiMn_2O_4$ electrode with 1M LiTDI, LiPDI and $LiPF_6$ in EC/DMC (50/50).

should be stressed that the upper limit (4.3 V) for these cycling tests is above that of commercial cells using the manganese spinel phase.

Finally, the power capability of these new salts was evaluated in the same type of cell configuration. The interpretation of such experiments should always be done with caution when comparing different cathode materials. Here, with a "fast" electrode (typical grain size ≈ 0.5 µm) material like $LiMn_2O_4$, there is no ambiguity that the signature curve in Figure 9 reflects the lithium throwing power of the electrolytes, again dependent of the total conductivity and of the transport number. The two salts compare quite well with $LiPF_6$, especially TDI with all the capacity available at 1C rate. For application, we also tested the wettability of LP30 and LiTDI/EC/DMC electrolytes with polyethylene separator and found that the contact surface was larger in case of LiTDI base electrolyte; the low surface energy being certainly brought by the CF3 group.

Conclusion

The two new salts based on the negatively charged imidazole ring rendered more dissociated by two" π" strongly electron-withdrawing cyano groups and one "σ" EWG CF_3– or C_2F_5– or namely TDI and PDI have been tested as substitutes for $LiPF_6$ in conventional carbonate solvents. The comparisons are quite positive, as these salts, totally covalent and not prone to hydrolysis, protect aluminium from corrosion up to potential that are not reached in conventional batteries. This is against conventional wisdom that links the formation of protective AlF_3 to facile release of F^- by the anion, which is not the case. There is no explanation yet for the formation of a protective film (or the preservation of the native Al_2O_3 film) in the presence of TDI or PDI. DCTA, the non-fluorinated analogue, also passivates aluminium, but its conductivity is only 40% of that of TDI.

On all tests, the two salts give good performances, and the only drawback is a slightly smaller conductivity and its consequence on the power capability. It must be stressed however that the optimum in lithium transport (EC/DMC ratio, concentration…) have not been sought for. Also, after several cycles, the growth of the SEI and its possible contamination by Mn ($LiMn_2O_4$) or Fe (low quality $FePO_4$) dissolved in the presence of $LiPF_6$ is the major source of impedance, not the electrolyte conductivity. In the last instance, the incineration of the battery in case of accidental fire would, with TDI, release only half of the HF compared to $LiPF_6$ and batteries with

these Hückel salts are expected to be safer, as immune from the dissociation equilibria occuring in the latter with the release of PF_5 and HF from its hydrolysis.

Acknowledgement:

The authors thank Matthieu Courty for the DSC/TGA experiment and Dr Murata (Nippon Shokubai, Japan) for providing a sample of LiDCTA to which our synthesis was compared.

References:

[1] S. Stewart & J. Newman, *J. Electrochem. Soc*. 155(2008) A458.

[2] Amer Hammami, Nathalie Raymond & Michel Armand , *Nature* 424 (6949) (2003) 635-636.

[3] C. Michot, M. Armand, M. Gauthier, Y. Choquette Patent WO/1998/029399 (1998).

[4] P. Johansson, H. Nilsson, P. Jacobson & M. Armand, *Physical Chemistry Chemical Physics* **6** (2004) 5.

[5] P. Johansson, S. Béranger, M. Armand, H. Nilsson, P. Jacobsson, *Solid State Ionics* **156** (1,2) (2003) 129-139.

[6] M. Egashira, B. Scrosati, M. Armand, S. Béranger, C. Michot, *Electrochemical and Solid-State Letters* **6 (4)** (2003) A71-A73.

[7] L. Niedzicki, G.Z. Żukowska, M. Bukowska, P. Szczeciński, S. Grugeon, S. Laruelle, M. Armand, S. Panero, B. Scrosati, M. Marcinek, W. Wieczorek, *Electrochim. Acta* 55 (2010) 1450-1454.

[8] L. Niedzicki, M. Kasprzyk, K. Kuziak, G.Z. Żukowska, M. Armand, M. Bukowska, M. Marcinek, P. Szczeciński, W. Wieczorek, *J. Power Sources* 192 (2009) 612-617.

[9] S. Altieri, D.P. Hinton, R.A. Byrd, *J. Am. Chem Soc*. 117 (1995) 7566-7567.

[10] J.-M. Tarascon, A. S. Gozdz, C. Schmutz, F. Shokoohi, and P. C. Warren, *Solid State Ionics*, **86** 49 (1996).

[11] J. Evans, Colin A. Vincent & P. G. Bruce, *Polymer* **28-13** (1987) 2324-232.

[12] W. Gorecki, P. Donoso, C. Berthier, M. Mali, J. Roos, D. Brinkmann & M. Armand, *Solid-State Ionics* **28-30** 1018 (1988).

[13] W. Gorecki, C. Roux, M. Clémancey, M. Armand, E. Belorizky, *Chem. Phys. Chem.* **3** (7) (2002) 620-625.